PROCEEDINGS, Twelfth Workshop on Geothermal Reservoir Engineering
Stanford University, Stanford, California, January 20-22, 1987
SGP-TR-109

TRACER BREAKTHROUGH TIME FOR THE RATE-PRESSURE DOUBLET

Will Menninger and Abraham Sageev

Stanford University

Stanford CA 94305

ABSTRACT

A pressure transient analysis method is presented for interpreting breakthrough time between a constant rate well and a constant pressure well. The wells are modeled as two line sources in an infinite reservoir where the first well injects at a constant pressure and the second well produces at a constant rate. The effects of transient pressure conditions, the distance between the wells, the flowrate, and the tracer injection time on breakthrough time are examined. The first arrival of injected fluid at the production well is significantly longer under transient condition than under steady state condition for the rate-pressure model when the injection pressure is equal to initial reservoir pressure. An injection pressure larger than initial reservoir pressure significantly reduces the breakthrough time, and may yield a breakthrough time significantly smaller than the breakthrough time for the steady state case.

INTRODUCTION

Pressure transient analysis methods are used to estimate reservoir properties so that exploitation schemes may be evaluated. Well-to-well tracer tests yield information about preferential flow paths and about reservoir heterogeneity. One of the important parameters in a well-to-well tracer test is the time of first arrival of the tracer at the production well, or the breakthrough time. The method presented in this paper permits the interpretation and design of a special case, which will be referred to as the rate-pressure doublet. In this two-well system, one well produces at a constant rate and the other well injects at a constant pressure. The two time dependent parameters in the rate-pressure doublet model are the pressure response of the producing well and the rate response of the injecting well. These parameters and ensuing equations will be described further in the Theory section.

A constant rate well is approximated as a line source, since the reservoir and the interwell distance are much larger than the finite radius of the well. The constant rate production or injection line source well has been used as a building block for calculating the response of various reservoir systems. *Theis* (1935) presented the line source pressure solution in an infinite domain. *Carslaw and Jaeger* (1960) and *Van Everdingen and Hurst* (1949) presented the pressure solution for a finite radius well in an infinite system. *Mueller and Witherspoon* (1965) showed the geometrical and time conditions under which the line source and the finite radius solutions are practically identical. They concluded that for observation wells located at a distance twenty times the wellbore radius the line source approximation is applicable. Also, this approximation is applicable for any observation well after a dimensionless time of ten.

Since the diffusivity equation describing the flow in the system is linear, superposition in space of constant rate line sources may be used. *Stallman* (1952) presented the superposition of two constant rate line sources replicating the effects of constant pressure or impermeable linear boundaries. In the same way, superposition of arrays of rate sources (*Kruseman and De Ridder* 1970, and *Ramey et al* 1973) were used to generate the effects of combinations of rectangular boundaries around a well. By using the method of superposition, the line source approximation, and fluid flow particle tracking, transient breakthrough time from the injecting well to the producing well is calculated for the rate-pressure well doublet. This transient breakthrough time is then compared to the analytical steady state solution for breakthrough time, and to the transient rate-rate solution for transient breakthrough time presented by *Menninger and Sageev* (1986).

THEORY

In the case of the steady state rate-rate well doublet, the velocity map is only a function of space, and is constant with respect to time. In the case of the transient rate-rate model, the velocity map is a function of space and time. This is true for the rate-pressure well doublet as well. In this section we present a summary of the various methods used for computing the velocity along the shortest stream line between the two wells (See Figure 1.) In the following derivations, we assume that the pressure behavior in the reservoir is governed by the diffusivity equation, and that the reservoir is homogeneous with isotropic properties. Also, we assume a unit mobility ratio and piston-like displacement.

We consider two independent well configurations in this section. In the first configuration, we have a well producing at a constant rate and an injection well that maintains a constant pressure equal to the initial pressure of the system, p_i. This configuration is termed the rate-pressure model, and was developed by *Sageev and Horne* (1983), and *Sageev and Horne* (1985a). The Second configuration includes a constant pressure injection well in an infinite reservoir, and is termed the constant pressure model. This configuration was described by *Carslaw and Jaeger* (1960), *Van Everdingen and Hurst* (1949), and by *Fetkovich* (1980). The superposition of the rate-pressure and the constant pressure models is presented in Figure 2, and was discussed by *Sageev and Horne* (1985b). The results of this superposition are presented in the Results section.

Velocity for the Rate-Pressure Model

The velocity for the rate-pressure model is a function of space and time. *Sageev and Horne* (1985a) presented the interference dimensionless pressure solution in Laplace

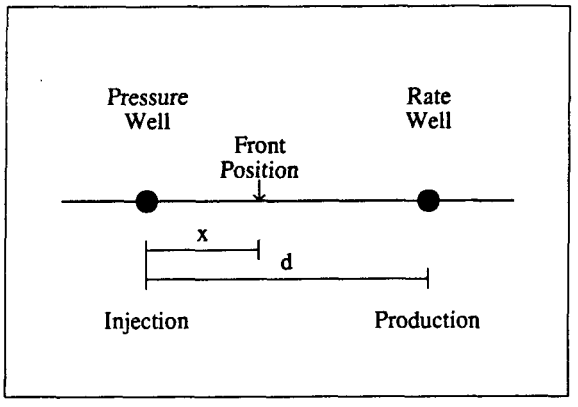

Figure 1: Schematic of a rate-pressure well doublet.

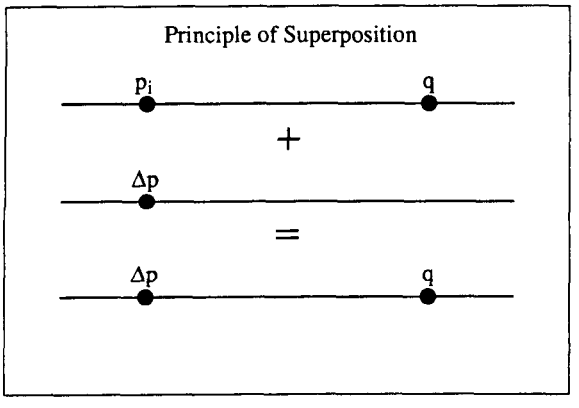

Figure 2: Schematic of the superposition for the rate-pressure well doublet.

space. Along the line between the two wells, the dimensionless Laplace pressure solution is:

$$\bar{p}_D = \frac{1}{s} \sum_{n=0}^{\infty} \varepsilon_n \left[I_n(x_D\sqrt{s})\, K_n(d_D\sqrt{s}) - \frac{I_n(\sqrt{s})\, K_n(d_D\sqrt{s})}{K_n(\sqrt{s})} K_n(x_D\sqrt{s}) \right] \quad (1)$$

where:
n = 0,1,2,3,.....
$\varepsilon_n = 1$ for n = 0
$\varepsilon_n = 2$ for n > 0
The variables are defined in the Nomenclature. The dimensionless Laplace spatial derivative of the pressure along the line between the two wells is:

$$\frac{\partial \bar{p}_D}{\partial x_D} = \frac{\sqrt{s}}{s} \sum_{n=0}^{\infty} \varepsilon_n \left[I_{n+1}(x_D\sqrt{s})\, K_n(d_D\sqrt{s}) + \frac{I_n(\sqrt{s})\, K_n(d_D\sqrt{s})}{K_n(\sqrt{s})} K_{n+1}(x_D\sqrt{s}) \right] \quad (2)$$

Finally, the velocity along the line between the two wells is:

$$V_x = \frac{-q}{2\pi\phi h r_w} \frac{\partial p_D}{\partial x_D} = \frac{-q}{2\pi\phi h r_w} L^{-1} \left\{ \frac{\partial \bar{p}_D}{\partial x_D} \right\} \quad (3)$$

Equation (2) involves an infinite summation on the order of modified Bessel functions, and is not readily inverted numerically to real time. Instead of using the Laplace velocity of Equation (3), we discretize the rate history at the constant pressure well, and use the superposition of constant rate line sources. This is described in the next two sections.

Velocity for the Constant Rate Case

The radial velocity field created by a constant rate well in an infinite reservoir is related to the derivative of pressure with respect to radius. In this study, the constant rate well is approximated by the *Theis* (1935) line source model. The dimensionless pressure solution for this model is:

$$p_D = -\frac{1}{2} E_i(-X) \quad (4)$$

where a positive dimensionless pressure is associated with pressures below the initial pressure p_i, and

$$X = \frac{r_D^2}{4t_D} \quad (5)$$

and the dimensionless terms are defined as:

$$t_D = \frac{kt}{\phi\mu c_t r_w^2} \quad (6)$$

and

$$r_D = \frac{r}{r_w} \quad (7)$$

The rest of the terms are defined in the Nomenclature. We are interested in computing the breakthrough time for the well doublet presented in Figure 1. The origin of the coordinate system is located at the injection well, hence, the tracer front moves along the straight line between the two wells. The distance between the two wells is denoted by d, and the distance between the location of the tracer front and the injection well is denoted by x. The Darcy velocity at a point x away from the injector caused by the constant rate production well is given by:

$$V_x = -\frac{k}{\mu} \frac{q\mu}{2\pi\phi k h r_w} \frac{\partial p_D}{\partial x_D} = \frac{-q}{2\pi\phi h r_w} \frac{\partial p_D}{\partial x_D} \quad (8)$$

The calculation of $\frac{\partial p_D}{\partial x_D}$ is performed using the formula for the derivative of the exponential integral:

$$\frac{dE_i(u)}{du} = \frac{1}{u} e^u \quad (9)$$

In terms of the coordinate system centered at the injection well, the dimensionless pressure and the spatial derivative of the dimensionless pressure are:

$$p_D = -\frac{1}{2} E_i \left[-\frac{\left[\frac{d-x}{r_w}\right]^2}{4t_D} \right] \quad (10)$$

$$\frac{\partial p_D}{\partial x_D} = \left[\frac{1}{\frac{d-x}{r_w}}\right] e^{-\frac{\left[\frac{d-x}{r_w}\right]^2}{4t_D}} \qquad (11)$$

The particle velocity, V_x, is calculated using Equations (8) and (11).

Velocity for the Constant Initial Pressure Well

Since the pressure at the injection well is constant and is equal to the initial pressure p_i, the time dependent variable is the injection rate. *Sageev and Horne* (1985b) presented the dimensionless Laplace rate solution for the injection well:

$$\bar{q}_D = \frac{-1}{\sqrt{s}}\left[I_1(\sqrt{s})K_0(d_D\sqrt{s}) + \frac{I_0(\sqrt{s})K_0(d_D\sqrt{s})}{K_0(\sqrt{s})} K_1(\sqrt{s})\right] \qquad (12)$$

where q_D is defined as:

$$q_D = \frac{q_{injection}}{q_{production}} \qquad (13)$$

The dimensionless rate at the injector starts with a value of zero and increases with time. At late time, the injection rate approaches the production rate and the dimensionless rate approaches unity. Figure 3, after *Sageev and Horne* (1985a), shows the rate response for various distances between the two wells. It takes a long time for the rate response at the constant pressure well to increase. The curves in Figure 3 were generated by numerically inverting Equation (12) using an algorithm developed by *Stehfest* (1970).

For a given system, we can generate the rate response of the constant pressure well using Equation (12). We discretize the time domain and assume that during a given time step, the injection rate is constant. Hence, after n time steps, we have n flow rates and we apply the method of superposition of constant rate line sources. The dimensionless pressure derivative at point x_D is related to the dimensionless rate by:

$$\frac{\partial p_D}{\partial x_D}(x_D,t_D) = \sum_i^n \frac{\Delta q_{Di}}{x_D} e^{-\frac{x_D^2}{4t_D - t_{Di}}} \qquad (14)$$

where Δq_{Di} and t_{Di} are the rates and beginning injection times of each hypothetical new well, respectively, and $x_D = x/r_w$. This method is visualized in Figure 4, where only two different Δq_i's are used. A Δq_i of 0.08 is used before tracer injection, and a Δq_i of 0.05 is used after tracer injection. With such a method for discretizing the injection rate into a set of constant rate changes, we can now calculate the velocity, $v(x,t)$, of any fluid particle. Combining this result with the one for the constant rate well, we can use superposition to calculate the velocity of any particle on the straight line path between the two wells, and thus we can use fluid flow front tracking to calculate the breakthrough time for the rate-pressure model.

Velocity for a Constant Pressure Well

In this section we present the velocity as a function of space and time caused by a constant pressure well in an

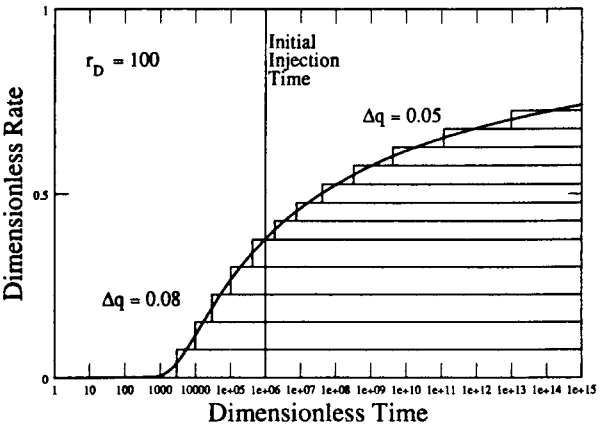

Figure 3: The dimensionless injection rate for various interwell distances. After *Sageev and Horne* (1985a).

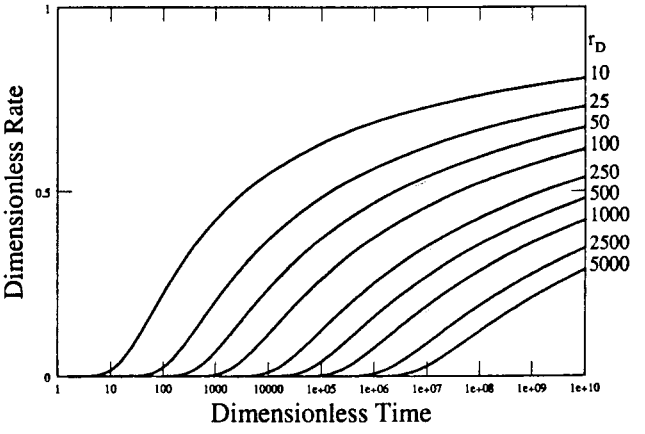

Figure 4: Discretized dimensionless rate curve, using different values of Δq before and after initial injection time.

infinite reservoir. The Laplace space solution, that was presented by *Carslaw and Jaeger* (1960), *Van Everdingen and Hurst* (1949), or by *Fetkovich* (1980) is:

$$\bar{p}_D = \frac{K_0(r_D\sqrt{s})}{sK_0(\sqrt{s})} \qquad (15)$$

where r_D is the dimensionless distance from the constant pressure source, and p_D is the dimensionless pressure, defined by

$$p_D = \frac{p - p_i}{\Delta p} \qquad (16)$$

where p_i is the initial reservoir pressure. Differentiating Equation (15) with respect to r_D yields:

$$\frac{\partial \bar{p}_D}{\partial r_D} = \frac{-\sqrt{s}K_1(r_D\sqrt{s})}{sK_0(\sqrt{s})} \qquad (17)$$

Equation (17) is numerically inverted to real space using the inversion algorithm developed by *Stehfest* (1970).

Hence, the velocity caused by the constant pressure well is:

$$V_x = -\frac{k\Delta p}{\mu r_w}\frac{\partial p_D}{\partial x_D} = -\frac{k\Delta p}{\mu r_w} L^{-1}\left\{\frac{\partial \bar{p}_D}{\partial x_D}\right\} \quad (18)$$

The Steady State Solution

The steady state solution to a rate-pressure well doublet is just the same as that for a rate-rate well doublet, however, approaching steady state is a much slower process for the rate-pressure configurations. This slow approach to steady state is due to the slow rate at which the constant pressure well approaches a steady state injection rate. From *Menninger and Sageev* (1986), the solution to the steady state breakthrough time for either rate-rate or rate-pressure doublets is:

$$t_{bt} = \frac{2\pi h\phi d^2}{6q} \quad (19)$$

This resulting breakthrough time for the steady state well doublet can now be compared to transient breakthrough times.

RESULTS

In this section, we describe the effects of the distance between the two wells, the rate of injection, the time of tracer injection, and the additional pressure drop at the injection well on the transient breakthrough time. In the first portion of the discussion, we concentrate on the rate-pressure model, where the injection well remains at the initial reservoir pressure p_i. In the second portion of the discussion, we consider the effects of the additional pressure rise at the injection well on the breakthrough time.

The Rate-Pressure Model

Consider a rate-pressure model with the following properties: $c_t = 6 \times 10^{-6}\ psi^{-1}$, $h = 20\ ft$, $k = 100\ md$, $\phi = 0.15$, $r_w = 0.5\ ft$, and $\mu = 1\ cp$. The effects of the rate of injection, q, the distance between the wells, d, and the initial tracer injection time, t_i, are examined in the next few figures. Figure 5 presents the effects of tracer injection time. Here, the time from tracer injection is graphed as a function of the position of the leading front of the tracer. The plot is cartesian. The top curve represents front tracking of a single constant rate producing well in an infinite reservoir, and the bottom curve represents a steady state doublet system. These extreme cases are used for comparison. We note that breakthrough time for the steady state case is at 120 days, and is much shorter than the breakthrough time for just a single constant rate producing well, that is 330 days. The second curve from the top represents a case where the tracer is injected at time zero into the rate-pressure doublet system with a breakthrough time of 160 days. As the the tracer injection time is delayed, the injection rate at the constant pressure well increases, and the breakthrough time decreases. However, even waiting for 10^{18} days before injecting the tracer, does not reduce the tracer breakthrough time to the steady state case (See Figure 5).

The top curve in Figure 5, representing the front position between the two wells caused by only the production well has an ever reducing slope. Hence, the velocity of the front increases with time along the particle flow path. The curves for the rate-pressure doublet have an inflection point. At short times after tracer injection, the slope of the curves is small, indicating a high velocity caused by the injection well. As the front moves away from the injector, the velocity decreases, and goes through a minimum about midway between the wells. As the front approaches the production well, the front velocity increases. The high front velocity at late time is caused by the large pressure gradients caused by the production well.

In Figure 6, we have the breakthrough times graphed as a function of the initial injection time in a semi-log format for the same example previously considered. As the tracer injection time is delayed, the breakthrough time decreases. The bars extending from the breakthrough time curve represent the time span for which the tracer front moves from the injection well to the production well along

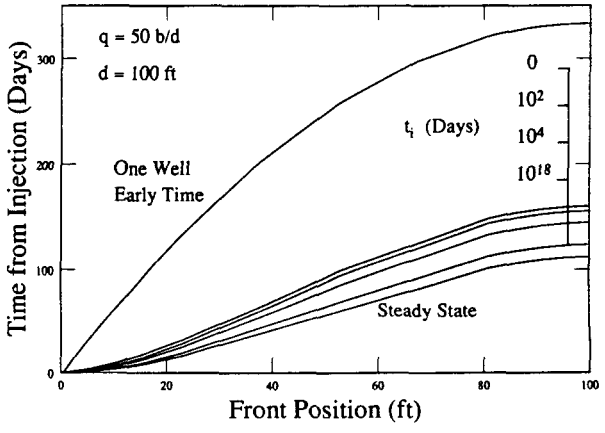

Figure 5: Front position for a rate-pressure doublet as a function of time for different tracer injection times. Reservoir parameters are: $\phi = 0.15$, $\mu = 1cp$, $c_t = 6\times10^{-6}\ psi^{-1}$, $h = 20\ ft$, $k = 100\ md$, $r_w = 0.5\ ft$.

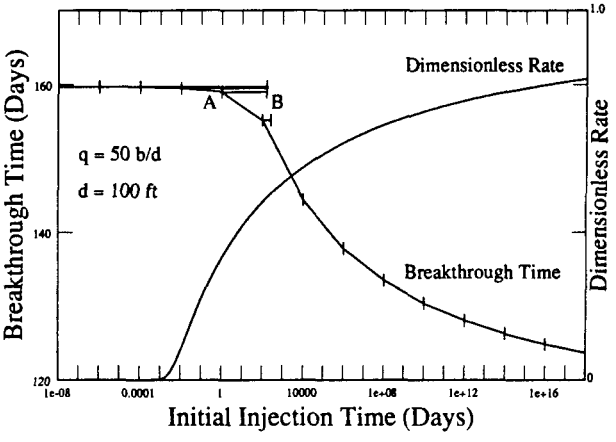

Figure 6: Breakthrough times and the dimensionless rate as a function of initial injection time. The bars represent the duration of the breakthrough time. Reservoir parameters are: $\phi = 0.15$, $\mu = 1cp$, $c_t = 6\times10^{-6}\ psi^{-1}$, $h = 20\ ft$, $k = 100\ md$, $r_w = 0.5\ ft$.

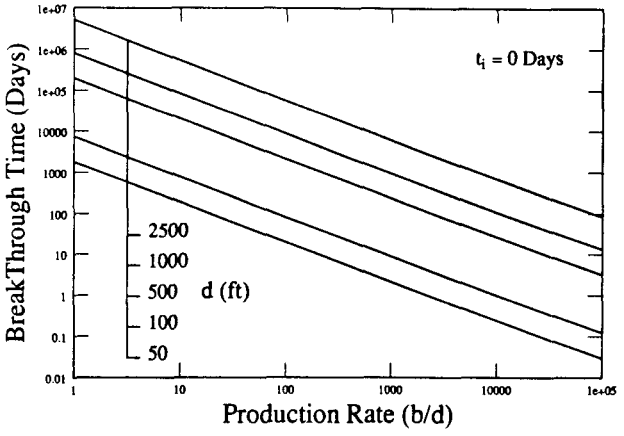

Figure 7: Breakthrough times as a function of production rate for various interwell distances with a zero tracer injection time. Reservoir parameters are: $\phi = 0.15$, $\mu = 1cp$, $c_t = 6\times10^{-6}\ psi^{-1}$, $h = 20\ ft$, $k = 100\ md$, $r_w = 0.5\ ft$.

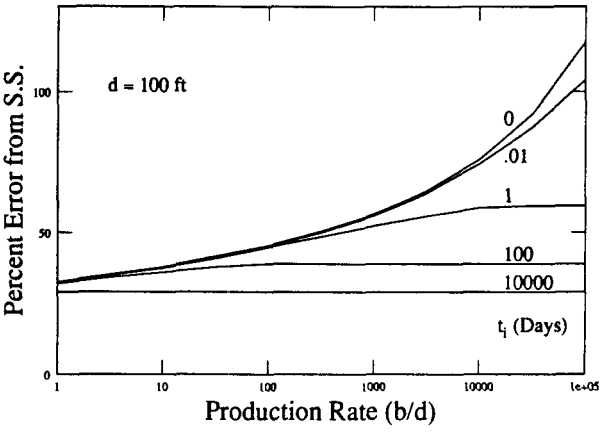

Figure 9: Percent error of the breakthrough times as a function of production rate for various tracer injection time and an interwell distance $d = 100\ ft$. Reservoir parameters are: $\phi = 0.15$, $\mu = 1cp$, $c_t = 6\times10^{-6}\ psi^{-1}$, $h = 20\ ft$, $k = 100\ md$, $r_w = 0.5\ ft$.

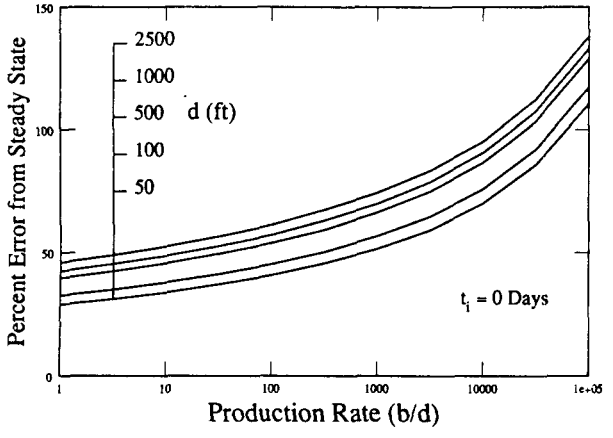

Figure 8: Percent error of the breakthrough times as a function of production rate for various interwell distances with a zero tracer injection time. Reservoir parameters are: $\phi = 0.15$, $\mu = 1cp$, $c_t = 6\times10^{-6}\ psi^{-1}$, $h = 20\ ft$, $k = 100\ md$, $r_w = 0.5\ ft$.

the straight line between them. Also the dimensionless rate of the constant pressure well is graphed in Figure 6. Points A and B represent the injection time and the arrival time respectively, for an initial tracer injection time of one day. As the initial tracer injection time increases, the average value of q_D under the bars representing the duration of the tracer test increases, and we get a corresponding reduction in breakthrough time. Hence, the time of tracer injection has a significant effect on tracer breakthrough time.

Figure 7 is a log-log presentation of the breakthrough time as a function of production rate for various values of the interwell distance. All the responses presented in Figure 7 are for the case where the tracer is injected at time zero, for the same reservoir properties discussed before. The lowermost curve in Figure 7 is for $d = 50\ ft$. As the production rate increases, the breakthrough time decreases. For a fixed production rate, the breakthrough time increases as the interwell distance increases.

In Figure 8, we see that the early time percent error from the steady state breakthrough times depends both on d and on q. We define the percent error as:

$$\%Error = \frac{t_{bt} - t_{bt,ss}}{t_{bt,ss}} \times 100 \qquad (20)$$

As the production rate increases or as the interwell distance increases, the deviation from the steady state solution increases. Figure 9 presents the combined effects of the production rate and the tracer injection time with a constant distance between the wells, $d = 100\ ft$. The dependence of the precent error on the flowrate q reduces as the initial injection time increases. As initial injection time increases, the rate of the constant pressure well changes less during the time that the tracer moves from the injector to the producer as demonstrated in Figure 6. For example, at $t_i = 100\ days$ (about where point B is in Figure 6), q_D changes less and less over the length of the bars, until the bars become so short that they look like a point on the dimensionless rate curve, and the rate of the constant pressure well can be considered constant over the duration of the breakthrough time. When $t_i = 10000\ days$, as Figure 9 shows, the precent error from the steady state case does not depend on the production rate.

since the shape of the dimensionless rate curves varies for each interwell distance, as shown in Figure 3, the error dependence on d does not disappear as t_i increases. As Figure 10 shows, the error curves change shape, but do not become horizontal, for the error depends on where t_i crosses each dimensionless rate curve (See Figure 3). For larger d, a constant t_i line crosses the rate curves in Figure 3 at lower rate values, yielding a transitionary flow period. Hence, the injection rate varies significantly during the tracer test, and the precent error from the steady state case increases. This is also demonstrated in Figure 11, that is a semi-log graph showing error dependence on initial injection time for varying d. The error levels off as t_i gets larger, and, as explained before, the injection rate varies less during the breakthrough process.

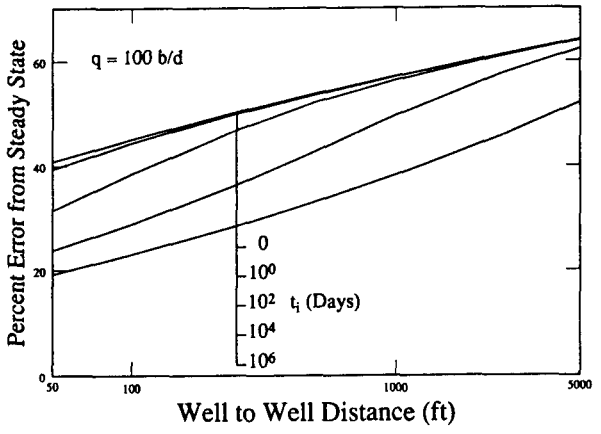

Figure 10: Percent error of the breakthrough times as a function of interwell distance and tracer injection time for a constant production rate $q = 100$ *b/d*. Reservoir parameters are: $\phi = 0.15$, $\mu = 1cp$, $c_t = 6\times10^{-6}\ psi^{-1}$, $h = 20\ ft$, $k = 100\ md$, $r_w = 0.5\ ft$.

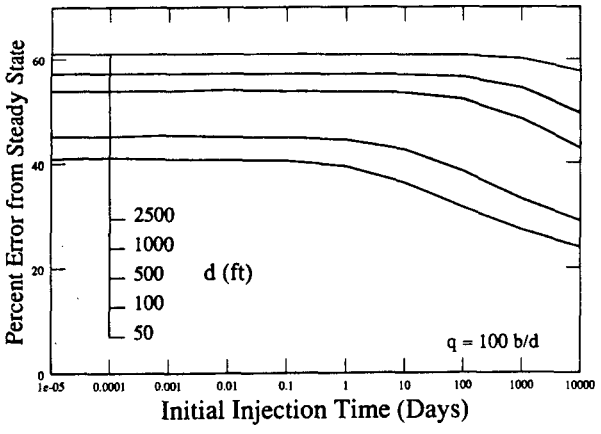

Figure 11: Percent error of the breakthrough times as a function of tracer injection time for various interwell distances and for a constant production rate $q = 100$ *b/d*. Reservoir parameters are: $\phi = 0.15$, $\mu = 1cp$, $c_t = 6\times10^{-6}\ psi^{-1}$, $h = 20\ ft$, $k = 100\ md$, $r_w = 0.5\ ft$.

The deviation of the breakthrough time for the rate-pressure model from the steady state breakthrough time is significant. This deviation is mainly attributed to the transient flow conditions around the production well, and to the slow response of the injection rate at the constant pressure well. Hence, the first injected tracer particle at the constant pressure well starts moving in the direction of the production well at a lower velocity in comparison to the steady state case, yielding a longer breakthrough time. One way in which to increase particle throughput and decrease breakthrough times in a rate-pressure doublet system is to create a pressure rise at the constant pressure well. This is described in the next section.

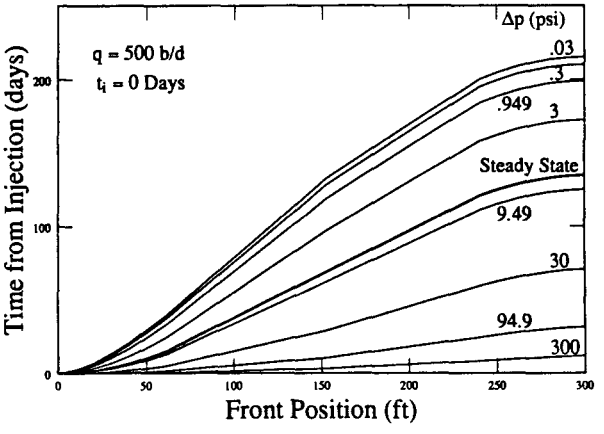

Figure 12: Front position for rate-pressure doublet as a function of pressure rise at the injection well for $q = 500$ *b/d* and zero tracer injection time. Reservoir parameters are: $\phi = 0.2$, $\mu = 0.5cp$, $c_t = 5\times10^{-6}\ psi^{-1}$, $h = 20\ ft$, $k = 50\ md$, $r_w = 0.3\ ft$.

The Rate-Pressure Doublet

The rate-pressure doublet differs from the rate-pressure model in the boundary condition at the constant pressure well. In the rate-pressure doublet, we impose a sudden pressure rise at the constant pressure well. Hence, the rate of injection at the constant pressure well is a function of the magnitude of the pressure rise imposed at the well, and of the response to the constant rate production well. The rate of injection caused by a constant pressure well in an infinite reservoir decreases with time, and was described by *Fetkovich* (1980). The rate of injection caused by the constant rate production well increases with time, as shown in Figure 3.

Figure 12 presents the time from tracer injection as a function of the tracer front position between the two wells for various pressure increases at the injection well, denoted by Δp. The reservoir parameters for the responses presented in Figure 12 are: $c_t = 5x10^{-6}\ psi^{-1}$, $h = 20ft$, $k = 50\ md$, $\phi = 0.2$, $r_w = 0.3\ ft$, $q = 500\ b/d$, $d = 100\ ft$, and $\mu = 0.5\ cp$. All the curves in Figure 12 are for a tracer injection time of zero. The highlighted curve in the middle represents the steady state rate-rate doublet case. The uppermost curve is for a small pressure rise at the injector of 0.03 psi, yielding a breakthrough time of about 60% larger than the steady state case. As the initial pressure rise at the injection well increases, the breakthrough time decreases significantly. For a Δp of 9.49 psi, the breakthrough time is just under the steady state case. For a Δp of 94.9 psi, the breakthrough time is mainly controlled by the injection well, and is about 20% of the steady state case.

Figure 13 presents similar curves as presented in Figure 12, with the tracer injection time at 10 days. The breakthrough times are slightly lower than the breakthrough times presented in Figure 12, and the main controlling parameter remains the magnitude of the pressure rise at the injection well.

The effects of the initial injection pressure rise at the injection well is summarized in Figure 14. In this figure, breakthrough times as a function of the injection pressure

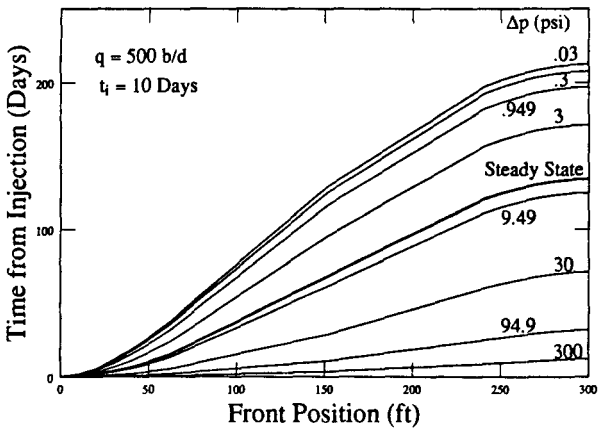

Figure 13: Front position for rate-pressure doublet as a function of pressure rise at the injection well for $q = 500$ *b/d* and for a tracer injection time of 10 days. Reservoir parameters are: $\phi = 0.2$, $\mu = 0.5cp$, $c_t = 5\times10^{-6}\ psi^{-1}$, $h = 20\ ft$, $k = 50\ md$, $r_w = 0.3\ ft$.

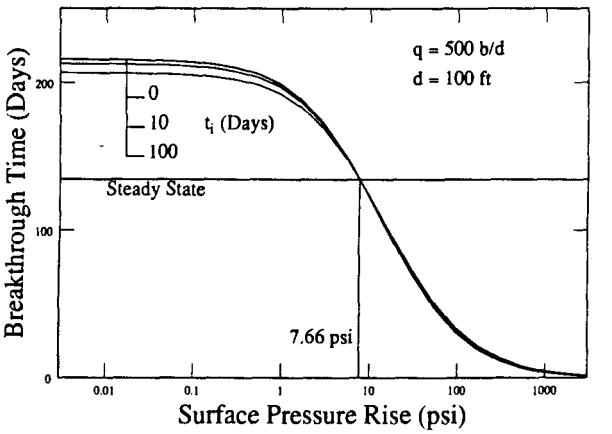

Figure 14: Breakthrough time as a function of pressure rise at the injection well for various tracer injection times, and $q = 500\ b/d$ and $d = 100\ ft$. Reservoir parameters are: $\phi = 0.2$, $\mu = 0.5cp$, $c_t = 5\times10^{-6}\ psi^{-1}$, $h = 20\ ft$, $k = 50\ md$, $r_w = 0.3\ ft$.

rise for various tracer injection times are presented. The horizontal line represents the steady state breakthrough time. For pressure rises smaller than 7.66 psi (for reservoir properties described in this section) breakthrough times are larger than the steady state breakthrough time by about 60%. The effects of the tracer injection time up to 100 days from the start of production is not significant. For pressure rises greater than 7.66 psi the breakthrough times for the rate-pressure doublet are smaller than for the steady state case. Large imposed pressure rises at the injection well dominate the tracer movement along the line between the two wells.

CONCLUSIONS

In the following conclusions we consider two well configurations: the rate-pressure model and the rate-pressure doublet. These two configurations differ in the imposed constant pressure, Δp, at the injection well. For the rate-pressure model $\Delta p = 0$ and for the rate-pressure doublet $\Delta p > 0$. In general, the rate-pressure model yields a breakthrough time larger than the steady state case. In the examples considered in this study, we observed that the breakthrough time may be 50%-100% larger than for the steady state case. The rate-pressure doublet may yield breakthrough times that are smaller or larger than the steady state case depending on the magnitude of the imposed pressure rise at the injection well. In the examples considered in this study, we found that the breakthrough time may be as low as 1/5 of the breakthrough time for the steady state case.

Rate-Pressure Model:

1. The breakthrough time reduces as the tracer injection time, and the production rate increase.
2. The percent error of the breakthrough time from the steady state case increases as the production rate and the interwell distance increase.
3. The percent error of the breakthrough time from the steady state case decreases as the tracer injection time increases.
4. The percent error of the breakthrough time from the steady state case for the rate-pressure model can be as high as 50%-100% for practical cases.

Rate-Pressure Doublet:

5. Small imposed pressure rises at the injection well yield breakthrough times similar to the breakthrough times for the rate-pressure model.
6. For small imposed pressure rises at the injection well, the breakthrough times are affected by the tracer injection time. As tracer injection time is increased, the breakthrough time decreases.
7. Large imposed pressure rises at the injection well dominate the space-time velocity of the tracer, and yield significantly smaller breakthrough times than the breakthrough times for the steady state model.
8. The effect of the tracer injection time is not significant when the imposed pressure rise at the injection well is large in comparison to the steady state pressure rise.

ACKNOWLEDGEMENTS

Financial support was provided by the Stanford Geothermal Program, DOE Contract No. DE-AT02-80SF11459, and by Stanford University.

NOMENCLATURE

E_i = Exponential Integral
I_n = Modified Bessel function, first kind, n'th order
K_n = Modified Bessel function, second kind, n'th order
V_x = Velocity in the x direction
X = Exponential Integral argument

c_t = total system compressibility
h = Formation thickness

k = Permeability
p = Pressure
p_D = Dimensionless pressure, $2\pi kh(p_i-p)/q\mu$
$\bar{p}_D$ = Laplace transformation of p_D
p_i = Initial pressure
Δp = Imposed injection well pressure rise
q = Volumetric rate
q_D = Dimensionless rate, $q(t)/q_{source}$
$\bar{q}_D$ = Laplace transformation of q_D
r = Radius
r_D = Dimensionless radius, r/r_w
r_w = Wellbore radius
s = Laplace variable
t = Time
t_{bt} = Breakthrough time
$t_{bt,ss}$ = Steady state breakthrough time
t_D = Dimensionless time, $kt/\phi\mu c_t r_w^2$
x = Distance from injector
x_D = Dimensionless distance, x/r_w

μ = Viscosity
ϕ = Porosity

REFERENCES

Carslaw, H.S. and Jaeger, J.C.:*Conduction of Heat in Solids*, 2nd ed. Oxford University Press, 1960.

Fetkovich, M.J.: "Decline Curve Analysis Using Type Curves," *J. Pet. Tech* (June 1980) 1065-1077.

Kruseman, G.P., and De Ridder, N.A.: "Analysis and Evaluation of Pumping Test Data," International Institute of Land Reclamation and Improvement, Wageningen, The Netherlands (1970).

Menninger, W., and Sageev, A.: "Breakthrough Time for the Source-Sink Well Doublet," Presented at the 11th Workshop on Geothermal Reservoir Engineering, Stanford, CA. (1986).

Mueller, T.D., and Witherspoon, P.A.: "Interference Effects Within Reservoirs and Aquifers," *J. Pet. Tech.* (Oct. 1965) 1803-1812.

Ramey, H.J., Jr., Kumar, A. and Gulati, M.S., *Gas Well Test Analysis Under Water Drive Conditions*, American Gas Association, Arlington, VA, (1973).

Sageev, A., and Horne, R.N.: "Pressure Transient Analysis of Reservoirs with Linear or Internal Linear Boundaries," SPE 12076, Presented at the 58th Annual Technical Conference and Exhibition, San Francisco, California (Oct. 1983).

Sageev, A., and Horne, R.N.: "Interference Between Constant Rate and Constant Pressure Wells," Geothermal Resources Council, *Transactions*, v. 9, Part II, 573-577. (1985a).

Sageev, A., and Horne, R.N.: "Interference Between Constant Rate and Constant Pressure Reservoirs Sharing a Common Aquifer," *Soc. Pet. Eng. J.*, 419-426 (1985b)

Stallman, R.W., "Nonequilibrium Type Curves Modified for Two-Well Systems", U.S. Geol. Surv., Groundwater Note 3, (1952).

Stehfest, H.: "Algorithm 368, Numerical Inversion of Laplace Transforms," *Communications of the ACM*, D-5 13, No. 1, 47-49, (Jan. 1970).

Theis, C.V., "The Relationship Between the Lowering of Piezometric Surface and Rate and Duration of Discharge of Wells using Groundwater Storage," Trans., AGU, 2, 519, (1935).

Van Everdingen, A.F. and Hurst, W.: "The Application of the Laplace Transformation Flow Problems in Reservoirs," *Trans.*, AIME (Dec. 1949) 186, 305-324.